

electron microscopy was done for 15 min under similar conditions with 3.75-fold higher protease and protein concentrations.

21. G. G. Glenner, *Prog. Histochem. Cytochem.* **13**, 1 (1981).

22. Aggregated protein or peptide suspensions were mixed with 0.1 volume of 2% (w/v) CR (Sigma) and, after 1 hour at 20°C, were centrifuged at 8500g for 30 s. The aggregates were washed twice with 100 μ l of water. Aggregates were suspended in an equal volume of water and 10 μ l was placed on a glass slide and allowed to dry. Excess CR was removed by washing with 90% ethanol. Samples were viewed by polarization microscopy using a Zeiss Axialfold microscope equipped with optimally aligned cross-polarizers.

23. W. E. Klunk, J. W. Pettegrew, D. J. Abraham, *J. Histochem. Cytochem.* **37**, 1293 (1989).

24. H. K. Edskes, V. T. Gray, and R. B. Wickner, *Proc. Natl. Acad. Sci. U.S.A.*, in press.

25. C.-Y. King *et al.*, *ibid.* **94**, 6618 (1997).

26. J. R. Glover *et al.*, *Cell* **89**, 811 (1997).

27. M. M. Patino, J.-J. Liu, J. R. Glover, S. Lindquist, *Science* **273**, 622 (1996).

28. G. G. Glenner *et al.*, *ibid.* **174**, 712 (1971).

29. After the Ni-NTA step, Ure2p aggregates were formed on dialysis against <0.15 M NaCl in 50 mM tris-HCl (pH 7.5). However, these aggregates were amorphous and had no filament structure.

30. Plasmid construction: a His₆-URE2 fusion was constructed by polymerase chain reaction (PCR) with primers (5'-CGCGGATCCAAAAAATGCATCACCATC-ACCATCACATGATGAATAACAACGGC-3') and (5'-GGAAGTGTCCGCGAATTCGTGGTGGGGTAAC-3'). The purified PCR product was digested with Bam HI and Sal I and ligated to Bam HI- and Xho I-treated pH7 vector (24) (derived from pRS425 and containing LEU2 and the ADH1 promoter). This construct (pKT18) was checked by sequencing. Strain 3947

(MAT α kar1 ure2 Δ ura2 Δ leu2 Δ ade5 Δ trp1 Δ pep4::HIS3 GAL+) carrying pKT18 (His₆-URE2 fusion) did not take up ureidosuccinate, showing that the URE2 fusion was functional. [URE3] could be cytotuded from strain 3310 [URE3-1] (MAT α kar1 arg1 [URE3]) into strain 3947 containing pKT18 showing that the fusion protein could assume the prion form. These clones, made [ure-o] by growth to single colonies on minimal medium containing 5 mM GuHCl, were used for purification of Ure2p.

31. R. W. Williams, *J. Mol. Biol.* **166**, 581 (1983); in *Enzyme Structure*, C. H. W. Hirs and S. N. Timasheff, Eds. (Academic Press, New York, 1986), vol. 130, pp. 311-331.

32. We thank P. McPhie for help with spectroscopy, G. Poy for synthetic peptides, L. Pannell for mass spectrometry, and H. Edskes for plasmid pH7.

3 December 1998; accepted 25 January 1999

A Glial-Neuronal Signaling Pathway Revealed by Mutations in a Neurexin-Related Protein

Li-Lian Yuan* and Barry Ganetzky†

In the nervous system, glial cells greatly outnumber neurons but the full extent of their role in determining neural activity remains unknown. Here the axotactin (*axo*) gene of *Drosophila* was shown to encode a member of the neurexin protein superfamily secreted by glia and subsequently localized to axonal tracts. Null mutations of *axo* caused temperature-sensitive paralysis and a corresponding blockade of axonal conduction. Thus, the AXO protein appears to be a component of a glial-neuronal signaling mechanism that helps to determine the membrane electrical properties of target axons.

Glial cells influence neural activity indirectly by insulating neurons and regulating their microenvironment, but they also have direct effects on neuronal signaling and plasticity (1). The molecules responsible for mediating

communication between neurons and glia are largely unknown.

Neurexins are a family of neuronal cell surface proteins with proposed roles in cell adhesion and intercellular signaling (2).

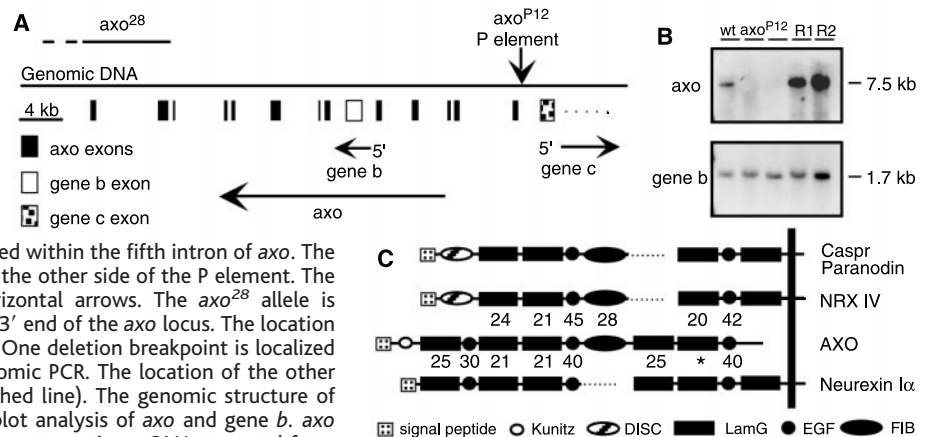
Three distinct genes encoding neurexins have been identified in vertebrates. Neurexins, together with the closely related NCP protein family [defined by *Drosophila* and human neurexin IV, along with rat contactin-associated protein (Caspr, also known as paranodin)], constitute a protein superfamily (2). Studies indicate that members of the NCP family are involved in neuronal-glial interactions in both vertebrates and invertebrates. *Drosophila* neurexin IV mutants (*nrx IV*) disrupt septate junctions and impair the blood-brain barrier (3). Vertebrate Caspr may also mediate glial-dependent insulation of axons (4). The protein binding domains in the

Neuroscience Training Program and Laboratory of Genetics, 445 Henry Mall, University of Wisconsin-Madison, Madison, WI 53706 USA.

*Present address: Division of Neuroscience, Baylor College of Medicine, Houston, TX 77030, USA.

†To whom correspondence should be addressed. E-mail: ganetzky@facstaff.wisc.edu

Fig. 1. Molecular analysis of the *axo* locus. (A) Genomic structure of the *axo* locus. The exon-intron boundaries of *axo* were determined from genomic sequence analysis. Three genes (*axo*, gene *b*, and gene *c*) are localized in the vicinity of the P-element insertion site as determined by Northern blot and cDNA analysis. The *axo* gene contains at least 13 exons that span more than 45 kb of genomic DNA. The P element (vertical arrow) is inserted 23 bases upstream of the first exon of *axo*. The entire transcript of gene *b* is nested within the fifth intron of *axo*. The transcript of gene *c* is located upstream of *axo* on the other side of the P element. The direction of each transcript is indicated by horizontal arrows. The *axo*²⁸ allele is associated with a deletion of at least 10 kb at the 3' end of the *axo* locus. The location of the deletion is indicated by the horizontal line. One deletion breakpoint is located between exons 11 and 12, as determined by genomic PCR. The location of the other breakpoint is not determined (indicated by a dashed line). The genomic structure of gene *c* is not completely mapped. (B) Northern blot analysis of *axo* and gene *b*. *axo* cDNA probes recognize a 7.5-kb band in the lane representing mRNA prepared from wild-type adult flies. This 7.5-kb band is undetectable in *axo*^{P12} mutants and is fully restored in two *axo*^{P12} revertants, *axo*^{P12-R1} (R1) and *axo*^{P12-R2} (R2). Complementary DNA probes from gene *b* recognize a 1.7-kb band. Neither this transcript nor the 4.2-kb transcript recognized by cDNA probes from gene *c* (not shown) is altered in the *axo*^{P12} mutant. (C) Diagram of the structural organization of AXO as compared with that of members of the neurexin superfamily. The other proteins represented are *Drosophila* neurexin IV (NRX IV), rat Caspr/paranodin, and rat neurexin I α (2-4). Gaps (dotted lines) are introduced into the sequences of the other proteins to maximize their alignment with the AXO sequence. The percent amino acid identity between the different domains in AXO and the corresponding domains in NRX IV or neurexin I α is shown. The asterisk indicates that the two domains are less than 20% identical. The cysteine-rich Kunitz-like domain is present only in AXO. In addition, all the other proteins except AXO contain a transmembrane domain. DISC, discoidin domain.



REPORTS

cytoplasmic tails of neuexins and NCPs enable members of the neuexin superfamily to provide a link between the extracellular en-

vironment and intracellular signaling pathways (2).

Identification of additional members of

the neuexin superfamily and analysis of their functions *in vivo* should help elucidate their biological significance. Here we report the genetic and molecular characterization of the *Drosophila axo* gene, which encodes a member of the neuexin superfamily expressed in glia but is also apparently required for normal axonal membrane excitability. *axo* was identified by isolation of a recessive P element-induced mutation, *axo^{P12}*, in a screen for temperature-sensitive paralytic mutations (5). A single P element at 64C1-3 on the polytene chromosomes was detected in *axo^{P12}*; its precise excision in rare revertants confirmed that it caused the mutant phenotype.

Genomic DNA flanking the element was cloned and used to identify the corresponding *axo* transcript (6) (Fig. 1A). Northern (RNA) blot analysis revealed a 7.5-kb transcript that is missing in *axo^{P12}* mutants but is restored in revertants (7) (Fig. 1B). The complete loss of a gene product in *axo^{P12}*, rather than the production of a thermolabile protein, is consistent with other temperature-sensitive paralytic mutants in *Drosophila* in which the elimination or reduced expression of various ion channels under all conditions renders the organism hypersensitive to the physiological effects of elevated temperatures (8, 9).

A set of overlapping cDNAs encompassing the entire *axo* transcript was isolated and sequenced (10). AXO contains several motifs, including an NH₂-terminal hydrophobic signal sequence followed by a consensus cleavage site, three cysteine-rich epidermal growth factor (EGF) repeats, five laminin G (Lam G) repeats, and a fibrinogen β/γ -like (FIB) segment. The arrangement of these domains, together with computer-based sequence alignments, identified AXO as a member of the neuexin superfamily (Fig. 1C). Several features distinguished AXO from other members of the superfamily: a Kunitz-like domain (11); the presence of both a Lam G domain (characteristic of neuexins) and a FIB domain (characteristic of NCPs) adjacent to the second EGF repeat; and the absence of a transmembrane domain, which suggests that AXO is secreted rather than membrane-associated (12).

Beginning at embryonic stage 13, *axo* transcripts were detected in the differentiating nervous system in wild-type but not in *axo^{P12}* embryos in a segmentally repeated pattern of discrete spots directly overlying the longitudinal axonal tracts (Fig. 2, A and C). This pattern was not coincident with neuronal cell bodies, which lie lateral and medial to the nerve bundles (13), but corresponded with the location of a subset of glial cells, including longitudinal glia and segmental boundary cells (14). The glial identity of these cells was confirmed by elimination of the *axo* signal in *gcm* (*glial cells missing*) embryos (15) (Fig. 2, C and D). This pattern of expression was

Fig. 2. Expression patterns of the *axo* transcript and encoded AXO protein. (A) In situ hybridization with an *axo* cDNA probe in whole-mount wild-type embryos (stage 13) oriented with anterior to the left. For methods, see (13). The top embryo shows a lateral view (ventral side down) and the bottom embryo shows a dorsal view. Arrow indicates the ventral ganglion; double-headed arrow indicates the nerve cord. The segmentally repeated pattern seen as a series of discrete spots in the ventral nerve cord is maintained in the third instar thoracic ganglion (B). Anterior is to the left. (C and D) Dissected embryonic ventral nerve cords, double-labeled by in situ hybridization with an *axo* cDNA probe (blue) and immunostained with the BP102 monoclonal antibody (orange), which stains axonal tracts (15). Anterior is at the top. In (C), the location of the *axo*-expressing cells relative to the axonal tracts suggests their identity as a subset of longitudinal glia. This control embryo, derived from the intercross of *gcm/CyO* males and females, is *gcm/CyO* in genotype. The nerve cord shown in (D) is from a *gcm/gcm* embryo from the same cross. *gcm* homozygous embryos are recognizable by the aberrant structure of their ventral nerve cords, revealed with the BP102 antibody. No *axo*-expressing cells are observed when glia are eliminated by the *gcm* mutation. (E) Immunostaining of a dissected wild-type nerve cord with a polyclonal antiserum to AXO. Anterior is to the left. In contrast to the distribution of the *axo* transcript seen in (A) and (C), the AXO protein is localized to longitudinal axon tracts (solid arrow) as well as to an axonal scaffold in the brain (open arrow). (F) Immunostaining of an *axo^{P12}* embryo with polyclonal antiserum to AXO. No staining is detectable. Scale bar, 50 μ m in (A), (B), (E), and (F); 20 μ m in (C) and (D).

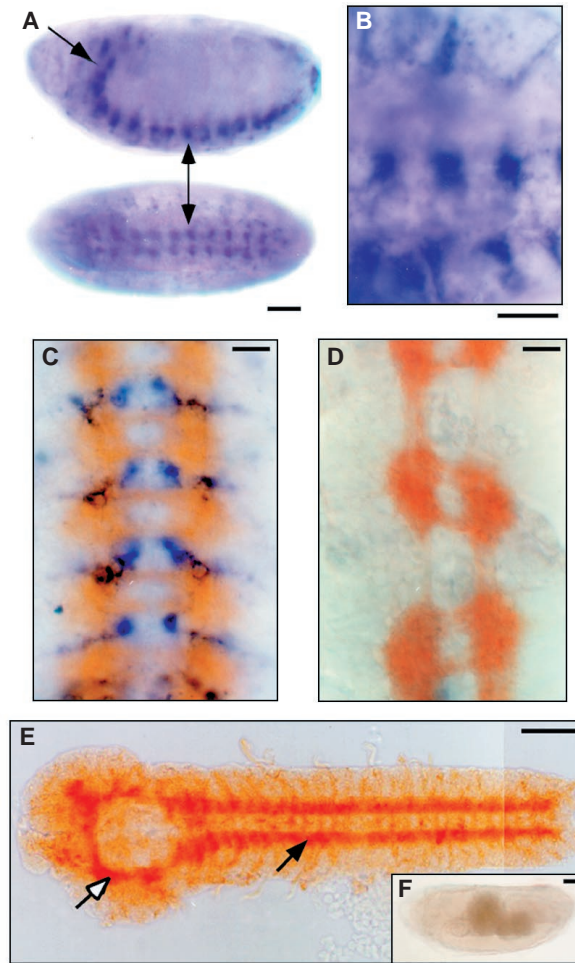
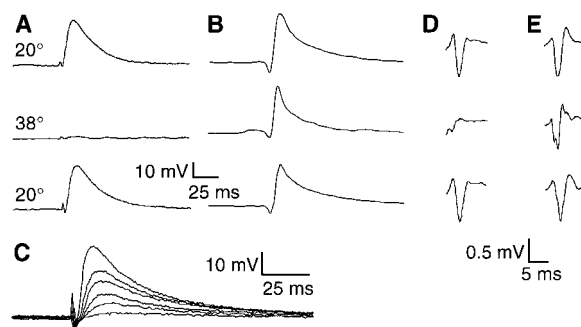


Fig. 3. Temperature-dependent failure of conduction in *axo*. (A) A representative set of recordings from one of the *axo^{P12}* larvae that showed a complete loss of the EJP at elevated temperature. At 20°C (top), the EJP appeared normal in amplitude and duration. However, after 10 min at 38°C (middle), the response could no longer be evoked. When the temperature returned to 20°C (bottom), the EJP fully recovered. (B) A representative set of recordings from a wild-type larva under the same conditions as in (A). In the wild-type larva, the EJP persisted at the elevated temperature for at least 20 min. (C) Graded electrotonic EJPs were still elicited in *axo^{P12}* larvae after the active response failed at 38°C by the positioning of the stimulating electrode closer to the nerve terminal and the use of stimuli of increasing intensity. After 10 min at 38°C, compound action potentials recorded with a suction electrode were severely diminished in *axo^{P12}* (D) but not in normal (E) larvae. Recovery was nearly complete upon return to room temperature.



maintained throughout the third larval instar. The distribution of the AXO protein (*I6*) differed from that of the *axo* transcript: AXO coincided with axonal tracts in the ventral nerve cord, brain, and parts of the peripheral nervous system (Fig. 2E). Thus, AXO appeared to be secreted from glia and subsequently localized to axonal tracts.

These results suggested that impairment of some aspect of neuronal development or function caused by loss of AXO resulted in a paralytic phenotype. Immunohistochemical studies of *axo* mutants indicated that development of the embryonic nervous system was normal, as were the number and distribution of synaptic boutons at the larval neuromuscular junction. Thus, the paralytic phenotype apparently involved a functional rather than a structural defect.

Excitatory junctional potentials (EJPs) were recorded at the larval neuromuscular junction (*I7*). At 20°C, the resting membrane potential and the amplitude and duration of evoked EJPs were normal in *axo^{P12}* larvae. However, EJPs were lost within 10 min at 38°C (in 15 out of 20 larvae) (Fig. 3A) (*I8*). During this interval, the threshold required to evoke EJPs increased until transmission failed completely. At 38°C, electrotonic stimulation still elicited the graded release of neurotransmitter in *axo^{P12}* larvae, demonstrating that both neurotransmitter release and postsynaptic response were apparently normal under these conditions (Fig. 3C). However, direct nerve recordings revealed a defect in axonal conduction. At 37°C, compound action potentials in mutant nerves were either lost or were reduced by more than 90% ($n = 10$), in contrast with wild-type nerves, in which no failure was seen ($n = 7$) (Fig. 3, D and E) (*I7*).

Defects in septate junctions in *Drosophila nrx IV* mutants result in loss of the blood-brain barrier and the failure of action potential in high [K⁺] bathing solutions. Temperature-dependent failure of nerve conduction in *axo^{P12}* larvae occurred even when larvae were bathed in low [K⁺] solutions, and failure was not exacerbated in high [K⁺] solutions. Thus, the blood-brain barrier was intact in *axo* mutants.

Taken together, the phenotypic and molecular properties of AXO suggest that it is a component of a glial-neuronal signaling pathway that is important in establishing the electrical properties of axonal membranes. We

have previously shown that a temperature-sensitive defect in axonal conduction is conferred by mutations in structural or regulatory genes that result in reduced numbers of sodium channels (*8*). Moreover, kinesin mutations in *Drosophila* also impair action potential propagation as an apparent consequence of reduced sodium and potassium channel density in axonal membranes (*19*). Consequently, we hypothesize that an *axo*-dependent signal is required for the normal expression, localization, or clustering of some set of ion channels. The aberrant expression or distribution of these channels in *axo* mutants would thus underlie the observed defect in nerve conduction at elevated temperatures. Recent work with vertebrate cell culture systems demonstrates that glia actively determine neuronal function by secreting factors that affect neuronal membrane excitability (*1, 20*). However, the identity of these factors is still unknown. AXO may be one such factor in *Drosophila*.

References and Notes

1. B. A. Barres, *J. Neurosci.* **11**, 3685 (1991); F. W. Pfrieger and B. A. Barres, *Science* **277**, 1684 (1997).
2. J. T. Littleton, M. A. Bhat, H. J. Bellen, *J. Cell Biol.* **137**, (1997); M. Missler and T. C. Sudhof, *Trends Genet.* **14**, 20 (1998); H. J. Bellen, Y. Lu, R. Beckstead, M. A. Bhat, *Trends Neurosci.* **21**, 444 (1998).
3. S. Baumgartner et al., *Cell* **87**, 1059 (1996).
4. E. Peles et al., *EMBO J.* **16**, 978 (1997); S. Einheber et al., *J. Cell Biol.* **139**, 1495 (1997); M. Menegoz et al., *Neuron* **19**, 319 (1997).
5. *axo^{P12}* homozygotes appeared normal at 20° to 22°C but became paralyzed within 3 min at 37° to 38°C. Full recovery occurred at 20° to 22°C within 7 to 8 min.
6. Genomic DNA flanking the P element insertion site was recovered by plasmid rescue [V. Pirrotta, in *Drosophila, A Practical Approach*, D. R. Roberts, Ed. (IRL Press, Oxford, 1986), pp. 83–110]. A group of genomic DNAs extending maximally 10 kb from the 5' end of the element and another group extending maximally 17 kb from the 3' end of the element were recovered. These genomic clones were used to screen an adult head cDNA library (T. Schwarz, Stanford University), and cDNAs were isolated representing three different transcription units encoding mRNAs of 1.7 kb, 4.2 kb, and 7.5 kb. Five additional gamma-ray-induced *axo* alleles were isolated by failure to complement the paralytic phenotype of *axo^{P12}*.
7. Northern blot analysis was performed as described [R. W. Ordway, L. Pallanck, B. Ganetzky, *Proc. Natl. Acad. Sci. U.S.A.* **91**, 5715 (1994)]. Five to 10 mg of polyadenylated RNA were loaded in each lane.
8. K. Loughney, R. Kreber, B. Ganetzky, *Cell* **58**, 1143 (1989); M. J. Kernan, M. I. Kuroda, R. Kreber, B. S. Baker, B. Ganetzky, *ibid.* **66**, 949 (1991).
9. N. Atkinson, G. Robertson, B. Ganetzky, *Science* **253**, 551 (1991); G. Feng, P. Deak, M. Chopra, L. M. Hall, *Cell* **82**, 1001 (1995); S. A. Titus, J. W. Warmke, B. Ganetzky, *J. Neurosci.* **17**, 875 (1997); X. Wang, E. R. Reynolds, P. Deak, L. M. Hall, *ibid.*, p. 882.

10. A single open reading frame of 5505 base pairs was found, beginning with a methionine codon preceded by a *Drosophila* consensus initiation sequence (AAAATG) [D. R. Cavener, *Nucleic Acids Res.* **15**, 1353 (1987)]. The stop codon is followed by a 1.9-kb untranslated tail that includes a potential polyadenylation signal.
11. M. Kunitz and J. H. Northrop, *J. Gen. Physiol.* **19**, 991 (1936); K. J. Lucchesi and E. Moczydlowski, *ibid.* **97**, 1295 (1991); H. Schweitz et al., *Proc. Natl. Acad. Sci. U.S.A.* **91**, 878 (1994).
12. Results from extensive polymerase chain reaction (PCR) analysis suggest that *axo* does not undergo any alternative splicing within the coding region. In contrast, hundreds of isoforms of mammalian neurexins, including some that are secreted, are generated by alternative splicing.
13. C.-S. Hong and B. Ganetzky, *J. Neurosci.* **14**, 5160 (1994).
14. C. S. Goodman and C. Q. Doe, in *The Development of Drosophila*, M. Bate and A. M. Arias, Eds. (Cold Spring Harbor Laboratory Press, Cold Spring Harbor, NY, 1993), p. 1131; K. Ito et al., *Roux's Arch. Dev. Biol.* **204**, 284 (1995).
15. B. W. Jones, R. D. Fetter, G. Tear, C. S. Goodman, *Cell* **82**, 1013 (1995); T. Hosoya, K. Takizawa, K. Nitta, Y. Hotta, *ibid.*, p. 1025.
16. A rat polyclonal antibody was raised against a bacterially expressed fusion protein corresponding to an extracellular domain of AXO (amino acids 410 through 643). The fusion protein was generated with the QIA expression system, purified on Ni-NTA resin (Qiagen), and further gel-purified for immunizing animals. For immunostaining, primary antibody was diluted 1:250, and rabbit anti-rat immunoglobulin G was diluted 1:1000.
17. Larval EJPs and nerve recordings were carried out according to standard methods [C. F. Wu, B. Ganetzky, L. Y. Jan, L. N. Jan, S. Benzer, *Proc. Natl. Acad. Sci. U.S.A.* **75**, 4047 (1978)]. The recording solution consisted of 2 mM KCl, 128 mM NaCl, 4 mM MgCl₂, 1 mM CaCl₂, 36 mM sucrose, and 5 mM Hepes (pH 7.2). The [K⁺] of high-K solution was modified to 40 mM, which is approximately the concentration of K⁺ found in *Drosophila* hemolymph [M. Ashburner, *Drosophila: A Laboratory Handbook* (Cold Spring Harbor Laboratory Press, Cold Spring Harbor, NY, 1989), p. 207].
18. In a small number of cases (5 out of 20 larvae), there was only a slight reduction (<20%) in EJP amplitude at 38°C. However, even in these larvae, transmission defects were apparent because there were many failures in response to a 5-Hz stimulus. In contrast, wild-type larvae and *axo^{P12}*-revertant larvae exposed to 38°C for up to 20 min showed no failure of EJPs and no change in the stimulus threshold in response to a 5-Hz train ($n = 8$).
19. M. Gho, K. McDonald, B. Ganetzky, W. M. Saxton, *Science* **258**, 313 (1992).
20. R. L. Wu and M. E. Barish, *J. Neurosci.* **14**, 1677 (1994); M. R. Kaplan et al., *Nature* **386**, 724 (1997).
21. We thank B. Jones and C. Goodman for providing the *gcm* strain; R. Kreber for excellent technical help; C.-S. Hong for advice and help on the initial phase of this project; C.-F. Wu, M.-L. Chen, and M. Stern for providing help and equipment for some experiments; and T. Littleton, G. Wilson, B. Anson, and C. Kung for comments on the manuscript. Supported by grants from NIH (GM43100 and NS15390) and Wyeth-Ayerst. This is paper number 3527 from the Laboratory of Genetics, University of Wisconsin, Madison.

13 October 1998; accepted 22 January 1999